

Fused cardiac hybrid imaging with coronary computed tomography angiography and positron emission tomography in patients with complex coronary artery anomalies

Christoph Gräni, MD | Dominik C. Benz, MD | Mathias Possner, MD |
Olivier F. Clerc, MD | Fran Mikulicic, MD | Jan Vontobel, MD | Julia Stehli, MD |
Tobias A. Fuchs, MD | Aju P. Pazhenkottil, MD | Oliver Gaemperli, MD |
Philipp A. Kaufmann, MD | Ronny R. Buechel, MD

Department of Nuclear Medicine, Cardiac Imaging, University Hospital Zurich, Zurich, Switzerland

Correspondence

Ronny R. Buechel, Cardiac Imaging, Department of Nuclear Medicine, University Hospital Zurich, Ramistrasse 100, 8091 Zurich, Switzerland.
Email: ronny.buechel@usz.ch

Christoph Gräni and Dominik C. Benz share the first authorship.

Abstract

Objective: To provide data on the value of fused cardiac hybrid imaging with coronary computed tomography angiography (CCTA) and positron emission tomography myocardial perfusion imaging (PET-MPI) in patients with complex coronary artery anomalies (CCAA).

Design/setting: This is a retrospective, single-center study.

Patients: Seven consecutive patients with CCAA (mean 57 ± 7 y, 86% were male) who underwent clinically indicated hybrid CCTA/PET-MPI between 2005 and 2015 in our clinic were included. The findings from both modalities and fused cardiac hybrid imaging were evaluated in these patients.

Results: Out of the seven patients with CCAA, two patients had Bland–White–Garland anomaly, two patients showed a coronary artery fistula, two patients showed a “single right,” and one patient showed a “single left” coronary artery. Semiquantitative fused hybrid CCTA/PET-MPI depicted inferolateral scar matching the territory of a nonanomalous vessel with significant concomitant coronary artery disease (CAD) in one patient only. In contrast, analysis of quantitative myocardial blood flow (MBF) as assessed by fused hybrid CCTA/PET-MPI revealed abnormally reduced flow capacities in the territories subtended by the anomalous vessels in 4 patients.

Conclusions: In this case series of middle-aged patients with CCAA, perfusion defects as assessed by semiquantitative PET-MPI were rare and attributable to concomitant CAD rather than to the anomalous vessel itself. By contrast, impaired MBF as assessed by quantitative hybrid CCTA/PET-MPI was revealed in the majority of patients in the vessel territories subtended by the anomalous coronary artery itself. Fused hybrid CCTA/PET-MPI incorporating information on morphology and on semiquantitative and quantitative myocardial perfusions may provide added value for the management of patients with CCAA.

KEYWORDS

coronary artery anomalies, coronary computed tomography, fused, hybrid, positron emission tomography myocardial perfusion

1 | INTRODUCTION

Complex coronary artery anomalies (CCAA) such as Bland–White–Garland syndrome, anomalous coronary artery origin from the opposite

sinus (ACAOS), “single right” or “single left” coronary arteries, and coronary artery fistulas occur with an incidence of 0.002%–1% in the adult population.^{1–3} Noninvasive coronary computed tomography angiography (CCTA) has become the primary modality in evaluating and

characterizing CCAA, as CCTA offers a higher accuracy and detection rate over invasive coronary angiography, echocardiography and magnetic resonance imaging.^{4–6} CCAA are considered to be associated with symptoms of myocardial ischemia, angina pectoris, dyspnea, palpitations, ventricular arrhythmia, congestive heart failure, syncope, and sudden cardiac death (SCD).^{2,7–10} Although standardized guidelines for the workup of CCAA are lacking, it has been suggested that a hybrid morphological and functional noninvasive imaging approaches, including CCTA and single photon emission computed tomography imaging myocardial perfusion imaging (SPECT-MPI), might be of added value for risk stratification and decision making in CCAA.^{10–16} SPECT-MPI, however, allows the assessment of myocardial perfusion on a semiquantitative basis (ie, assessing the relative differences of normalized myocardial radiotracer uptake) only. In contrast, positron emission tomography myocardial perfusion imaging (PET-MPI) expands current diagnostic capabilities of SPECT-MPI through its ability to additionally offer absolute quantitation of myocardial blood flow (MBF). It is well known that the assessment of quantitative MBF by PET-MPI exerts an added value for risk stratification and provides prognostic information for patients with subclinical coronary artery disease (CAD), balanced triple vessel CAD, cardiac transplant, and microvascular dysfunction in cardiomyopathies.^{17–21} However, the assignment of territories to the correct subtending coronary artery is challenging. In fact, it has been shown that the so-called standard distribution of myocardial perfusion territories does not correspond with individual true anatomy in more than half of the patients with normal coronary anatomy,²² a rate that can be assumed to be much higher in patients with CCAA. Thus, it may be hypothesized that hybrid imaging with fusion of CCTA and semiquantitative and quantitative PET-MPI offers an added value for patients with CCAA.

2 | METHODS

2.1 | Patient population and follow-up

We retrospectively identified all consecutive patients with CCAA revealed by CCTA who underwent additional clinically indicated PET-MPI between March 2005 and May 2015 in our clinic and recorded the findings. Aside from morphological information on the coronary anatomy as offered by CCTA, we evaluated the following parameters derived from PET MPI: semiquantitative perfusion, hyperemic absolute MBF, coronary flow reserve (CFR), and relative flow reserve (RFR). Fused hybrid imaging using CCTA datasets and semiquantitative as well as quantitative MBF parameters was performed for each patient. Clinical data, symptoms, and outcome data were assessed, and follow-up was obtained by performing telephone interviews and reviewing electronic patient records. Major adverse cardiovascular events (MACE) were defined as cardiac death, myocardial infarction, revascularization or anomalous vessel-related cardiac surgery.

2.2 | CCTA imaging

CCTA was performed on multislice CT scanners (LightSpeed VCT XT and Revolution CT; GE Healthcare, Waukesha, WI, USA) according to

the current guidelines and as previously described.^{23,24} Prior to examination, all patients received 2.5 mg isosorbiddinitrate sublingually (Isoket; Schwarz Pharma, Monheim, Germany), and up to 30 mg metoprolol (Beloc Zok; AstraZeneca, London, United Kingdom) was administered intravenously if heart rate per minute was >65 in order to obtain optimal image quality.²⁴ Iodixanol (Visipaque 320, 320 mg/mL; GE Healthcare) was injected into an antecubital vein followed by 50 mL saline solution.

2.3 | PET imaging

Cardiac ¹³N-ammonia PET was performed using a 1-d rest/stress or stress/rest protocol. Stress was pharmacologically induced using adenosine at a standard rate (0.14 mg/min/kg) over 7 min, as previously reported.¹⁸ All patients received a 700–900 MBq injection of ¹³N-ammonia into a peripheral vein during 10 s as a slow bolus. Images were acquired in two-dimensional mode on a PET or PET/CT scanner (Advance, Discovery LS, Discovery DSTX, and Discovery VCT; GE Healthcare), with a field of view between 14.6 and 15.7 cm. Dynamic acquisitions of the emission scans were performed using a standard protocol consisting of 9×10 , 6×15 , 3×20 , and 1×900 s frames. Transmission scan for photon attenuation correction was performed with low-dose CT attenuation correction (nongated, tube voltage 140 kV, tube current 120–150 mA, and slice thickness 3.75–4.75 mm).^{18,25}

Regional ¹³N-ammonia uptake was assessed using the 17-segment model and the semiquantitative scoring system of defect severity and extent, as recommended by the American Society of Nuclear Cardiology.²⁶ Quantitative MBF was determined using the PMOD software package (version 3.7; PMOD Technologies Ltd., Zurich, Switzerland) developed and validated at our institution.²⁷ A spherical region of interest was placed into the blood pool of the left ventricle. Myocardial and blood pool time-activity curves were generated from the dynamic frames and corrected for radioisotope decay. MBF was estimated by model fitting of the blood pool and myocardial time-activity curves²⁸ correcting for partial volume and spillover, as previously described.²⁹ CFR was calculated as the ratio of hyperemic to resting MBF, and CFR ≥ 2.0 was considered normal.³⁰ From the 17 segment model relative and absolute MBF in segments corresponding to anomalous and remote, nonanomalous vessels without CAD were assessed for the calculation of RFR. RFR was defined as the ratio of hyperemic MBF in the area of the target vessel (anomalous vessel) to hyperemic MBF in a normally perfused area (nonanomalous vessel without CAD),³¹ and a RFR of ≥ 0.78 was considered normal.³² In two-dimensional scatter plots integrating hyperemic MBF and CFR of territories perfused by anomalous versus nonanomalous vessels in the same patient with superimposed thresholds for normal, reduced flow capacity or definite ischemia as proposed by Johnson and Gould³³ were drawn.

2.4 | Hybrid imaging

Semiquantitative and quantitative datasets from PET-MPI were fused with CCTA datasets on a dedicated workstation (Advantage

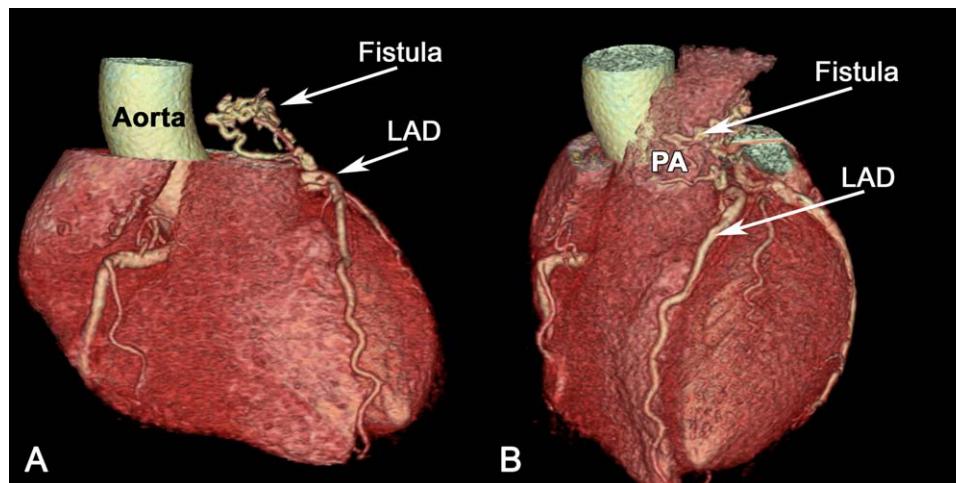


FIGURE 1 CCTA (A lateral view, B anterior view) reveals a fistula from the left anterior descending artery (LAD) to the pulmonary artery (PA). CCTA, coronary computed tomography angiography; PET-MPI, positron emission tomography myocardial perfusion imaging

Workstation 4.3; GE Healthcare) using a commercially available software tool (CardIQ Fusion; GE Healthcare), as previously described in detail.³⁴ A matched semiquantitative CCTA/PET-MPI fused imaging finding was defined as a reversible (ischemia) or fixed (scar) PET-MPI defect in a territory subtended by an anomalous vessel and/or a stenotic coronary artery (defined as narrowing of the coronary luminal diameter $\geq 50\%$).

2.5 | Statistical analysis

All statistical analyses were performed using SPSS Statistics 22 (IBM Corporation, Armonk, NY, USA). Data are reported as median \pm interquartile range (IQR; 25th–75th percentile), or mean \pm standard deviation, or percentages as appropriate.

2.6 | Ethics

The study conforms to the principles outlined in the Declaration of Helsinki and was evaluated and approved by the local ethics committee (KEK-ZH-Nr. 2015-0235). The need for informed written consent was waived.

3 | RESULTS

3.1 | Imaging results

We identified seven patients with CCAA who underwent both CCTA and PET-MPI. The mean age was 57 ± 7 years, and 86% were male. Two patients (28%) had Bland–White–Garland syndrome with one anomalous left coronary from the pulmonary artery (ALCAPA) (ie, patient 1) as previously published by our group¹² and one anomalous right coronary from the pulmonary artery (ARCAPA) (ie, patient 2). Two patients (28%) showed a single right coronary artery, that is, one patient with a subpulmonic course (between the aorta and the right ventricular outflow tract) of the left anterior descending artery (ie, patient 3) and one patient with a retroaortic course of the left coronary artery and an interarterial course of a septal branch (ie patient 4). One patient (14%) showed a single left coronary artery with an intramural and interarterial course of the right coronary artery (RCA) (ie, patient 5), and two patients (28%) showed a fistula from the left anterior descending artery (LAD) connecting to the pulmonary artery (ie patients 6 and 7) (Figure 1). Patient's characteristics and description of

TABLE 1 Patient's characteristics and types of anomaly

Patient no	Age	Gender	Symptoms	Type of anomaly	Origin of anomalous vessel	Course of anomalous vessel	Termination of anomalous vessel
1	56	f	Palpitations	ALCAPA	LM of PA	Normal	Normal
2	48	m	Palpitations	ARCAPA	RCA of PA	Normal	Normal
3	61	m	Typical angina	Single right	LM of RCS	Subpulmonic	Normal
4	55	m	Typical angina	Single right	LM of RCS	Interarterial	Normal
5	57	m	Typical angina	Single left	RCA of LCS	Interarterial	Normal
6	70	m	Syncope	Fistula LAD to PA	Normal	–	A. Pulm
7	52	m	Atypical angina	Fistula LAD to PA	Normal	–	A. Pulm

ALCAPA, anomalous left coronary from the pulmonary artery; ARCAPA, anomalous right coronary from the pulmonary artery; LAD, left anterior descending coronary artery; LCS, left coronary sinus; LM, left main artery; PA, pulmonary artery; RCA, right coronary artery; RCS, right coronary sinus.

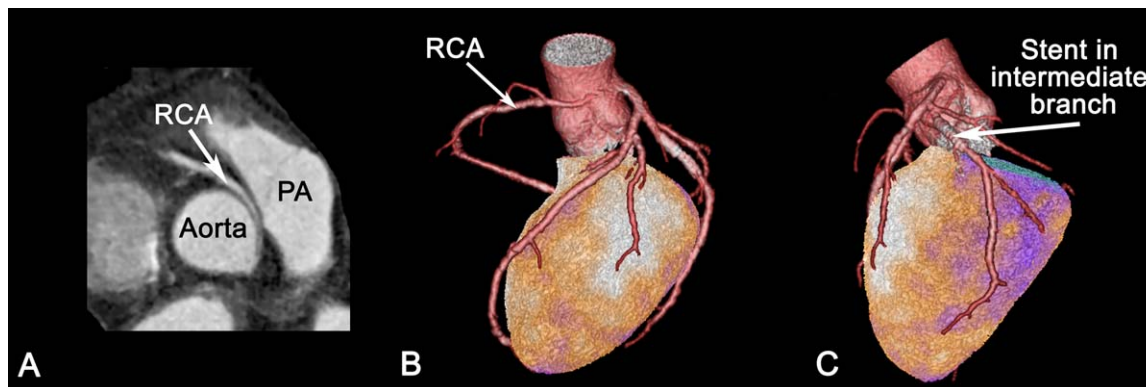


FIGURE 2 Fused CCTA/PET-MPI of a patient with a single left coronary artery. CCTA revealed a single left coronary artery (ie, patient 5) with an intramural and interarterial course of the anomalous right coronary artery (A). Fused CCTA/PET-MPI (using the stress dataset) showed an inferolateral scar matching the perfusion territory of the previous stented nonanomalous intermediate branch with concomitant CAD (B and C). CCTA, coronary computed tomography angiography; PET-MPI, positron emission tomography myocardial perfusion imaging

coronary artery anomalies are given in Table 1. Symptoms on referral were angina (43%), followed by palpitations (28%), atypical angina (14%), and syncope (14%). CCTA revealed concomitant CAD in two patients (28%, ie, patients 4 and 5). Semiquantitative PET-MPI revealed perfusion defects only in the patient with a single left coronary artery (ie, patient 5) with a scar in the inferolateral wall. Fused hybrid CCTA/PET-MPI revealed that the scar in the inferolateral wall was subtended by a previously stented coronary vessel with concomitant CAD (Figure 2).

Hyperemic MBF in anomalous vessel compared to the remote nonanomalous vessel were lower in all patients (see Table 2 and Figure 3), represented as a RFR <1.0 , except in a single patient (ie, patient 7) with a fistula. However, RFR was only pathologically reduced (ie, ≤ 0.78) in the two patients with Bland-White-Garland syndrome (ie, patients 1 and 2). Similarly, CFR of the anomalous vessel was lower in all patients compared to the remote non-anomalous vessel, except in the patient with single right coronary artery (ie, patient 4) and the patient with a fistula (ie, patient 7). Of note, in the patient with single right coronary artery (ie, patient 4), CFR with 1.94 was also slightly reduced in the segments corresponding to the distal part of the nonanomalous RCA with concomitant CAD, compared to

the other, nonanomalous vessel segments. Also in the patient with single left coronary artery (ie, patient 5), the nonanomalous vessels with concomitant CAD showed an impaired CFR. Only in the patient with ALCAPA (ie, patient 1), CFR was reduced in the anomalous vessel (1.40), and also to a lesser extent, in the remote, nonanomalous vessel (1.47) (see Figure 4). As the patient with single left coronary artery (ie, patient 5) showed left coronary circulation dominance of the nonanomalous vessel, MBF of the anomalous vessel (ie, RCA) could not be calculated.

In Figure 5, two-dimensional scatter plots of hyperemic MBF and CFR with superimposed thresholds for normal, reduced flow capacity or definite ischemia show that 83% (5 out of 6) of the patients showed a minimally to moderate reduced flow capacity in myocardial territories subtended by the anomalous vessels compared to the remote non-anomalous vessel for each patient.

3.2 | Outcome

During a median follow-up of 54 months (IQR 1–108), two patients (29%) experienced MACE. The patient with ALCAPA (ie, patient 1) suffered acute myocardial infarction after 41 months and hemi-arterial switch

TABLE 2 Quantitative PET-MPI analysis of anomalous and nonanomalous vessels

Patient no.	Anomalous vessel hyperemic MBF (mL/min/g)	Anomalous vessel CFR	Remote nonanomalous vessel hyperemic MBF (mL/min/g)	Remote nonanomalous vessel CFR	RFR
1	1.46	1.40	2.62	1.47	0.56
2	1.77	1.49	2.55	2.03	0.69
3	2.13	2.62	2.42	2.89	0.88
4	1.76	2.38	2.15	2.27	0.82
5	-	-	1.30	1.52	-
6	2.25	2.36	2.44	2.42	0.92
7	5.50	4.44	5.09	4.38	1.08

CFR, coronary flow reserve; MBF, myocardial blood flow; RFR, relative flow reserve.

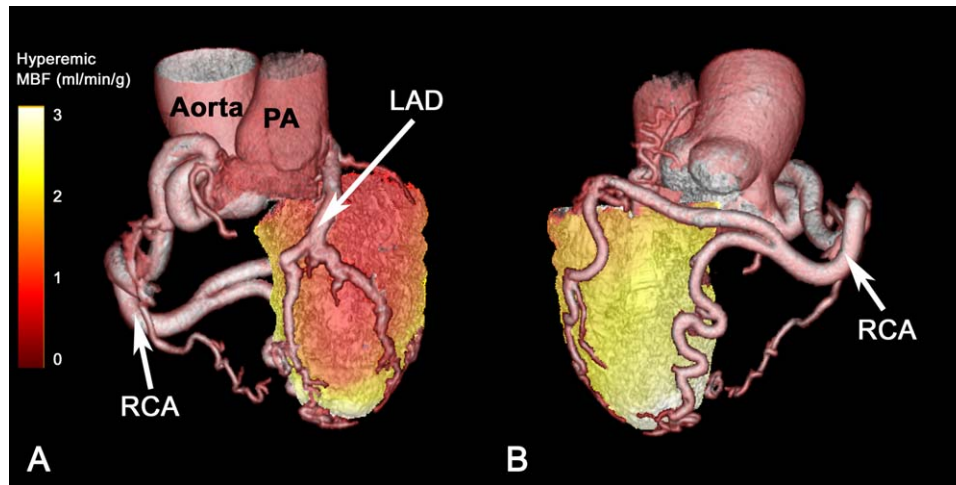


FIGURE 3 Fused CCTA/PET-MPI including quantitative hyperemic MBF of patient 1 with Bland–White–Garland syndrome (ie, ALCAPA: anomalous left anterior descending artery origin from the pulmonary artery). On panel (A), impaired hyperemic MBF in the territory of the anomalous vessel (ie, LAD) can be seen compared to normal hyperemic MBF of the nonanomalous vessel perfusion territory of the RCA on panel (B). CCTA, coronary computed tomography angiography; LAD, left anterior descending artery; MBF, myocardial blood flow; PA, pulmonary artery; PET-MPI, positron emission tomography myocardial perfusion imaging; RCA, right coronary artery

operation was performed after 72 months due to progressive dyspnea. The patient with single right coronary artery (ie, patient 4) underwent revascularization of the RCA after 1 month due to progressive angina pectoris.

4 | DISCUSSION

To the best of our knowledge, this is the first case series assessing the impact of CCAA on myocardial perfusion through fused hybrid CCTA/PET-MPI, integrating coronary morphology and semiquantitative and

quantitative perfusion parameters. In our study, semiquantitative perfusion defects (ie, ischemia and scar) were found in a single patient who had concomitant obstructive CAD in the vessel subtending the perfusion defect. In contrast, quantitative perfusion analysis revealed a reduced hyperemic MBF and a reduced CFR in almost all patients with CCAA in the anomalous vessels compared to a remote, nonanomalous vessel.

4.1 | Bland–White–Garland syndrome

A steal-phenomenon by reversed flow in the coronary artery into the pulmonary artery caused by decreased pulmonary artery pressure after

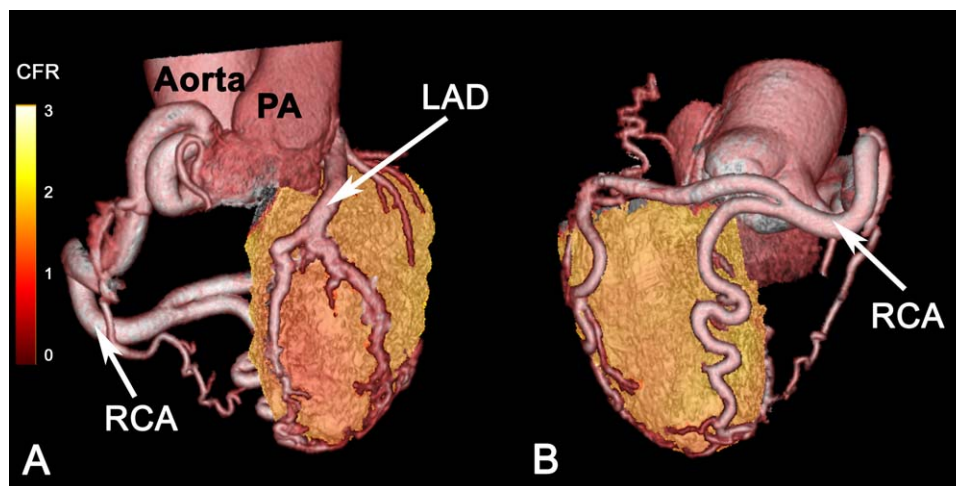


FIGURE 4 Fused CCTA/PET-MPI including coronary flow reserve of patient 1 with Bland–White–Garland syndrome (anomalous left anterior descending artery origin from the pulmonary artery). On panel (A), CFR in the territory of the anomalous vessel (ie, LAD) perfusion is impaired to a greater extent compared to the nonanomalous vessel perfusion territory of the right coronary artery on panel (B). CCTA, coronary computed tomography angiography; CFR, coronary flow reserve; LAD, left anterior descending artery; MBF, myocardial blood flow; PA, pulmonary artery; RCA, right coronary artery; PET-MPI, positron emission tomography myocardial perfusion imaging

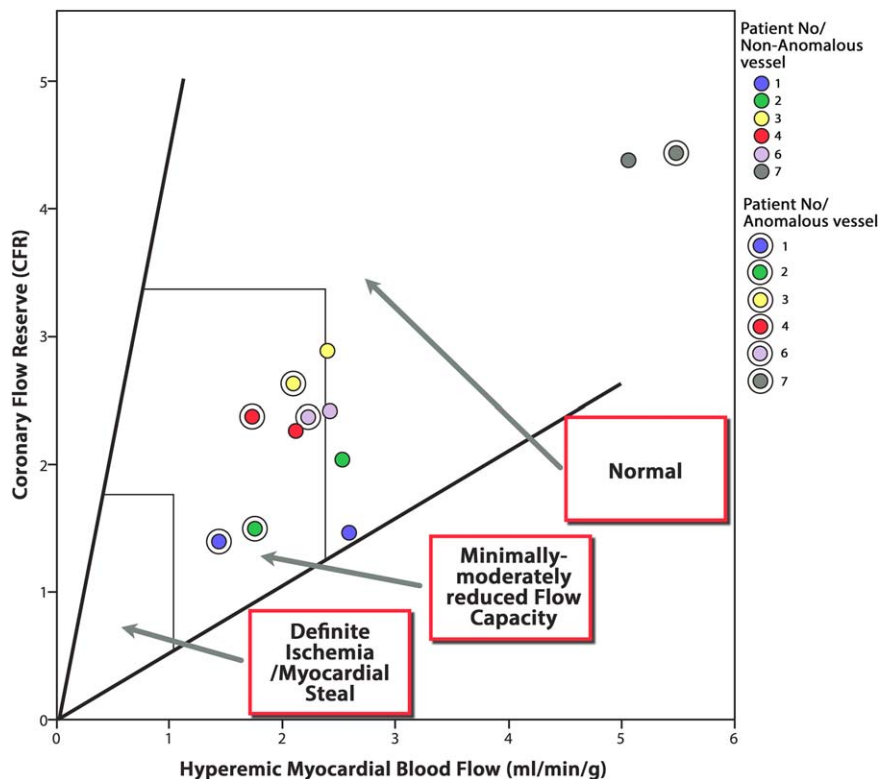


FIGURE 5 Two-dimensional scatter plots integrating hyperemic MBF and CFR of anomalous vessels versus nonanomalous vessel are depicted for each patient with superimposed thresholds for normal, reduced flow capacity or definite ischemia as proposed by Johnson and Gould (33). A total of 83% (5 out of 6) of the patients (ie, patients 1, 2, 3, 4, and 6) showed a minimally to moderate reduced flow capacity in the territories perfused by the anomalous vessels compared to the remote nonanomalous vessel in the same patient. As the patient with single left coronary artery (ie, patient 5) showed left coronary circulation dominance of the nonanomalous vessel, hyperemic MBF of the anomalous vessel could not be calculated and therefore patient 5 is not represented. CFR, coronary flow reserve; MBF, myocardial blood flow

birth is suggested to be underlying mechanism for perfusion defects in Bland–White–Garland patients undergoing SPECT-MPI.^{35–37} There is evidence that noninvasive quantitative perfusion imaging allows for estimation of fractional flow reserve (FFR) through calculation of RFR.³² As RFR of 0.78 has been suggested as the cutoff value for the lower limit of normal³². The two patients with Bland–White–Garland syndrome (ie, patients 1 and 2) showed abnormal RFR in our case series. Interestingly, in both patients with Bland–White–Garland syndromes, not only RFR but also CFR was reduced in the anomalous vessel, suggesting that quantitative MBF assessment by quantitative PET allows for the detection of a presumed steal-phenomenon in Bland–White–Garland syndrome.

4.2 | Coronary artery fistula

Similarly, and even in small coronary pulmonary artery fistulas, a steal-phenomenon may cause hypoperfusion and reduction of MBF distally of the affected coronary artery, as has been demonstrated using FFR in invasive coronary angiography.^{15,38} In-line with this study, one patient with coronary pulmonary artery fistula showed mildly reduced RFR and CFR in the present study. Interestingly, however, another patient (ie, patient 7) with coronary artery fistula did not show reduced CRF distally to the involved LAD compared to the remote nonanomalous ves-

sel and it was the only patient without a RFR <1. It can be hypothesized that—due to the rather small size of the fistula—the competitive shunting flow through the fistula to the pulmonary artery, compared to the antegrade flow to the distal LAD may not markedly increase during stress perfusion, and therefore, the fistula is hemodynamically insignificant. Although steal-phenomenon were described also in small coronary artery fistulas, others suggested that a true fistula is characterized by a distinct ectatic vascular segment that exhibits fistulous flow and is connected to two vascular territories with large pressure differences. Small coronary artery fistulas with long vascular channels may present with high vascular resistance, allowing only limited blood flow to the pulmonary artery, and may therefore not confer hemodynamical relevance.^{39,40}

4.3 | Anomalous origin of the coronary artery from the opposite sinus

Hyperemic MBF was mildly reduced in one case of ACAOS variant in the myocardium matching the territory subtended by the anomalous coronary artery. Moreover, hyperemic MBF was lower compared to the remote segments with an RFR of 0.82. This is in line with a report by Lim et al. who demonstrated that in a patient with ACAOS the invasively measured FFR of the interarterial variant of the vessel was

reduced from 0.96 to 0.87 with adenosine and to 0.86 during a dobutamine challenge.⁴¹ In some cases, even ischemia of territories corresponding to anomalous ACAOS vessels have been demonstrated using SPECT imaging.^{11,16,41} In contrast, we have recently demonstrated that myocardial ischemia caused by ACAOS per se seems exceedingly rare in middle-aged patients with ACAOS and is more likely attributable to concomitant CAD.¹³ With this regard, fused hybrid CCTA/SPECT-MPI proofed a valuable noninvasive tool to discriminate the impact of ACAOS from concomitant CAD on myocardial ischemia.¹³ Similarly, in the present study, hybrid CCTA/PET-MPI imaging allowed for such discrimination in one patient with ACAOS and concomitant CAD (ie, patient 5). In the same patient and also in the patient with single right coronary artery (patient 4), PET-MPI did not show ischemia but revealed that CFR was reduced in the territory subtended by the distal part of a nonanomalous vessel with concomitant CAD. Of note, out of the ACAOS patients, only the patient with “single right” coronary artery (ie, patient 3) and a subpulmonic course of the anomalous vessel had normal hyperemic MBF in the anomalous vessel and also a normal, and similar CFR compared to the remote nonanomalous vessel. This finding is of particular interest as it supports the presumption that the subpulmonic course of the anomalous vessel is rather a benign variant and that the anomalous vessel is normally perfused also under stress conditions.^{42–44}

The present case series extends our limited knowledge by demonstrating that perfusion defects as assessed by semiquantitative PET-MPI due to CCAA per se are rather rare and are much more likely attributable to concomitant CAD. However, hyperemic MBF, CFR, and RFR are of additional value as they offer a more accurate and sensitive diagnostic tool in evaluating these patients. In fact, impairment of absolute MBF as demonstrated by quantitative PET-MPI was seen in more than half of CCAA patients in our small cohort. Of note, a number of studies have shown that impaired hyperemic MBF and CFR as assessed by quantitative PET-MPI are powerful independent risk factors for cardiac death.^{18,19,21,45} Indubitably, larger studies are needed to evaluate whether quantitative assessment of myocardial perfusion through PET-MPI confers an added prognostic value in a population with CCAA. Nevertheless, due to the fact that the standard distribution models of myocardial perfusion territories are not applicable in patients with CCAA, our results suggest that fused hybrid imaging may constitute a valuable tool in this setting as it allows discrimination of CCAA from CAD in impaired myocardial perfusion. It may, therefore, be hypothesized that hybrid fused CCTA/PET-MPI offers a beneficial value for risk stratification in patients with CCAA.

5 | LIMITATIONS

The sample of patients studied in the present case series is small. However, while CCAA are extremely rare and availability of CCTA/PET-MPI fused imaging is limited, our findings are hypothesis-generating for larger multicenter studies. Nevertheless, due to the small sample size, extrapolation from our results should be made only with caution.

6 | CONCLUSIONS

In this case series of middle-aged patients with CCAA, perfusion defects as assessed by semiquantitative PET-MPI were rare and attributable to concomitant CAD rather than to the anomalous vessel itself. In contrast, impaired MBF as assessed by quantitative hybrid CCTA/PET-MPI was revealed in the majority of patients in the vessel territories subtended by the anomalous coronary artery itself. Fused hybrid CCTA/PET-MPI incorporating information on morphology and on semiquantitative and quantitative myocardial perfusion may provide added value for the management of patients with CCAA.

CONFLICT OF INTEREST

All authors have the following to disclose: The University Hospital of Zurich holds a research contract with GE Healthcare.

CONTRIBUTORS

Christoph Gräni, Dominik C. Benz, Philipp A. Kaufmann, and Ronny R. Buechel were responsible for the conception, design, analysis, interpretation of the data, and drafting of the article. Mathias Possner, Olivier F. Clerc, Fran Mikulicic, Jan Vontobel, Julia Stehli, Tobias A. Fuchs, Aju P. Pazhenkottil, and Oliver Gaemperli were involved in the acquisition of data and drafting of the article. All authors read and approved the final article.

REFERENCES

- Angelini P. Coronary artery anomalies: an entity in search of an identity. *Circulation* 2007;115(10):1296–1305.
- Loukas M, Germain AS, Gabriel A, John A, Tubbs RS, Spicer D. Coronary artery fistula: a review. *Cardiovasc Pathol* 2015;24(3):141–148.
- Yau JM, Singh R, Halpern EJ, Fischman D. Anomalous origin of the left coronary artery from the pulmonary artery in adults: a comprehensive review of 151 adult cases and a new diagnosis in a 53-year-old woman. *Clin Cardiol* 2011;34(4):204–210.
- Ghadri JR, Kazakauskaitė E, Braunschweig S, et al. Congenital coronary anomalies detected by coronary computed tomography compared to invasive coronary angiography. *BMC Cardiovasc Disord* 2014;14:81
- Kang JW, Seo JB, Chae EJ, et al. Coronary artery anomalies: classification and electrocardiogram-gated multidetector computed tomographic findings. *Semin Ultrasound CT MR* 2008;29(3):182–194.
- Zeina AR, Blinder J, Sharif D, Rosenschein U, Barmer E. Congenital coronary artery anomalies in adults: non-invasive assessment with multidetector CT. *Br J Radiol* 2009;82(975):254–261.
- Camarda J, Berger S. Coronary artery abnormalities and sudden cardiac death. *Pediatr Cardiol* 2012;33(3):434–438.
- Frommelt PC. Congenital coronary artery abnormalities predisposing to sudden cardiac death. *Pacing Clin Electrophysiol* 2009; 32(suppl 2): S63–S66.
- Seon HJ, Kim YH, Choi S, Kim KH. Complex coronary artery fistulas in adults: evaluation with multidetector computed tomography. *Int J Cardiovasc Imaging* 2010;26(suppl 2):261–271.
- Warnes CA, Williams RG, Bashore TM, et al. ACC/AHA 2008 guidelines for the management of adults with congenital heart

- disease: a report of the American College of Cardiology/American Heart Association Task Force on Practice Guidelines (Writing Committee to Develop Guidelines on the Management of Adults With Congenital Heart Disease). Developed in Collaboration With the American Society of Echocardiography, Heart Rhythm Society, International Society for Adult Congenital Heart Disease, Society for Cardiovascular Angiography and Interventions, and Society of Thoracic Surgeons. *J Am Coll Cardiol* 2008;52(23):e143-e263.
- [11] De Luca L, Bovenzi F, Rubini D, Niccoli-Asabella A, Rubini G, De Luca I. Stress-rest myocardial perfusion SPECT for functional assessment of coronary arteries with anomalous origin or course. *J Nucl Med* 2004;45(4):532-536.
- [12] Ercin E, Gamperli O, Kaufmann P, Eberli FR. Bland-White-Garland syndrome: extensive collaterals prevent ischaemia. *Eur Heart J* 2007;28(14):1672.
- [13] Grani C, Benz DC, Schmied C, et al. Hybrid CCTA/SPECT myocardial perfusion imaging findings in patients with anomalous origin of coronary arteries from the opposite sinus and suspected concomitant coronary artery disease. *J Nucl Cardiol* 2015 Dec 28 [Epub ahead of print].
- [14] Gunaydin S, Gokgoz L, Unlu M, et al. Bland-White-Garland syndrome in an adult. Case report and review of diagnostic and predictive strategies. *Scand Cardiovasc J* 1997;31(2):105-109.
- [15] Said SA, Nijhuis RL, Akker JW, et al. Unilateral and multilateral congenital coronary-pulmonary fistulas in adults: clinical presentation, diagnostic modalities, and management with a brief review of the literature. *Clin Cardiol* 2014;37(9):536-545.
- [16] Uebles C, Groebner M, von Ziegler F, et al. Combined anatomical and functional imaging using coronary CT angiography and myocardial perfusion SPECT in symptomatic adults with abnormal origin of a coronary artery. *Int J Cardiovasc Imaging* 2012;28(7):1763-1774.
- [17] Fukushima K, Javadi MS, Higuchi T, et al. Prediction of short-term cardiovascular events using quantification of global myocardial flow reserve in patients referred for clinical ⁸²Rb PET perfusion imaging. *J Nucl Med* 2011;52(5):726-732.
- [18] Herzog BA, Husmann L, Valenta I, et al. Long-term prognostic value of ¹³N-ammonia myocardial perfusion positron emission tomography added value of coronary flow reserve. *J Am Coll Cardiol* 2009;54(2):150-156.
- [19] Murthy VL, Naya M, Foster CR, et al. Improved cardiac risk assessment with noninvasive measures of coronary flow reserve. *Circulation* 2011;124(20):2215-2224.
- [20] Schelbert HR. Positron emission tomography measurements of myocardial blood flow: assessing coronary circulatory function and clinical implications. *Heart* 2012;98(7):592-600.
- [21] Ziadi MC, Dekemp RA, Williams KA, et al. Impaired myocardial flow reserve on rubidium-82 positron emission tomography imaging predicts adverse outcomes in patients assessed for myocardial ischemia. *J Am Coll Cardiol* 2011;58(7):740-748.
- [22] Schindler TH, Magosaki N, Jeserich M, et al. Fusion imaging: combined visualization of 3D reconstructed coronary artery tree and 3D myocardial scintigraphic image in coronary artery disease. *Int J Card Imaging* 1999;15(5):357-368. discussion 69-70.
- [23] Abbara S, Arbab-Zadeh A, Callister TQ, et al. SCCT guidelines for performance of coronary computed tomographic angiography: a report of the Society of Cardiovascular Computed Tomography Guidelines Committee. *J Cardiovasc Comput Tomogr* 2009;3(3):190-204.
- [24] Buechel RR, Husmann L, Herzog BA, et al. Low-dose computed tomography coronary angiography with prospective electrocardiogram triggering: feasibility in a large population. *J Am Coll Cardiol* 2011;57(3):332-336.
- [25] Koepfli P, Hany TF, Wyss CA, et al. CT attenuation correction for myocardial perfusion quantification using a PET/CT hybrid scanner. *J Nucl Med* 2004;45(4):537-542.
- [26] Machac J, Bacharach SL, Bateman TM, et al. Positron emission tomography myocardial perfusion and glucose metabolism imaging. *J Nucl Cardiol* 2006;13(6):e121-e151.
- [27] Siegrist PT, Gaemperli O, Koepfli P, et al. Repeatability of cold pressor test-induced flow increase assessed with H(2)(15)O and PET. *J Nucl Med* 2006;47(9):1420-1426.
- [28] Muzik O, Beanlands RS, Hutchins GD, Mangner TJ, Nguyen N, Schwaiger M. Validation of nitrogen-13-ammonia tracer kinetic model for quantification of myocardial blood flow using PET. *J Nucl Med* 1993;34(1):83-91.
- [29] Hutchins GD, Schwaiger M, Rosenspire KC, Krivokapich J, Schelbert H, Kuhl DE. Noninvasive quantification of regional blood flow in the human heart using N-13 ammonia and dynamic positron emission tomographic imaging. *J Am Coll Cardiol* 1990;15(5):1032-1042.
- [30] Camici PG, Crea F. Coronary microvascular dysfunction. *N Engl J Med* 2007;356(8):830-840.
- [31] De Bruyne B, Baudhuin T, Melin JA, et al. Coronary flow reserve calculated from pressure measurements in humans. Validation with positron emission tomography. *Circulation* 1994;89(3):1013-1022.
- [32] Stuijzand WJ, Uusitalo V, Kero T, et al. Relative flow reserve derived from quantitative perfusion imaging may not outperform stress myocardial blood flow for identification of hemodynamically significant coronary artery disease. *Circ Cardiovasc Imaging* 2015;8(1):
- [33] Johnson NP, Gould KL. Integrating noninvasive absolute flow, coronary flow reserve, and ischemic thresholds into a comprehensive map of physiological severity. *JACC Cardiovasc Imaging* 2012;5(4):430-440.
- [34] Gaemperli O, Schepis T, Kalff V, et al. Validation of a new cardiac image fusion software for three-dimensional integration of myocardial perfusion SPECT and stand-alone 64-slice CT angiography. *Eur J Nucl Med Mol Imaging* 2007;34(7):1097-1106.
- [35] Cowie MR, Mahmood S, Ell PJ. The diagnosis and assessment of an adult with anomalous origin of the left coronary artery from the pulmonary artery. *Eur J Nucl Med* 1994;21(9):1017-1019.
- [36] Kanamaru H, Karasawa K, Ichikawa R, et al. Dual myocardial scintigraphy mismatch in an infant with Bland-White-Garland syndrome. *Int J Cardiol* 2009;135(1):e1-e3.
- [37] Katsuragi M, Yamamoto K, Tashiro T, Nishihara H, Toudou K. Thallium-201 myocardial SPECT in Bland-White-Garland syndrome: two adult patients with inferoposterior perfusion defect. *J Nucl Med* 1993;34(12):2182-2184.
- [38] Harle T, Kronberg K, Elsasser A. Coronary artery fistula with myocardial infarction due to steal syndrome. *Clin Res Cardiol* 2012;101(4):313-315.
- [39] Angelini P. Coronary-to-pulmonary fistulae: what are they? What are their causes? What are their functional consequences? *Texas Heart Institute Journal* 2000;27(4):327-329.
- [40] Yew KL, Ooi PS, Law CS. Functional assessment of sequential coronary artery fistula and coronary artery stenosis with fractional flow reserve and stress adenosine myocardial perfusion imaging. *J Saudi Heart Assoc* 2015;27(4):283-285.
- [41] Lim MJ, Forsberg MJ, Lee R, Kern MJ. Hemodynamic abnormalities across an anomalous left main coronary artery assessment:

- evidence for a dynamic ostial obstruction. *Catheter Cardiovasc Interv* 2004;63(3):294–298.
- [42] Leberthson RR, Dinsmore RE, Bharati S, et al. Aberrant coronary artery origin from the aorta. Diagnosis and clinical significance. *Circulation* 1974;50(4):774–779.
- [43] Nath H, Singh SP, Lloyd SG. CT distinction of interarterial and intraseptal courses of anomalous left coronary artery arising from inappropriate aortic sinus. *Am J Roentgenol* 2010;194(4):W351–W352.
- [44] Yamanaka O, Hobbs RE. Coronary artery anomalies in 126,595 patients undergoing coronary arteriography. *Catheter Cardiovasc Diag* 1990;21(1):28–40.
- [45] Neglia D, Michelassi C, Trivieri MG, et al. Prognostic role of myocardial blood flow impairment in idiopathic left ventricular dysfunction. *Circulation* 2002;105(2):186–193.

How to cite this article: Gräni C, Benz DC, Possner M, Clerc OF, Mikulicic F, Vontobel J, Stehli J, Fuchs TA, Pazhenkottil AP, Gaemperli O, Kaufmann PA, and Buechel RR. Fused cardiac hybrid imaging with coronary computed tomography angiography and positron emission tomography in patients with complex coronary artery anomalies. *Congenital Heart Disease*. 2017;12:49–57. doi:10.1111/chd.12402.